Research Paper

Overexpression of long noncoding RNA ANRIL inhibits phenotypic switching of vascular smooth muscle cells to prevent atherosclerotic plaque development *in vivo*

Da-Jun Hu[2], Zhen-Yu Li[1,3], Yuan-Ting Zhu[1,3], Chuan-Chang Li[1,3]

[1]Department of Geriatric Medicine, Xiangya Hospital, Central South University, Changsha 410008, China
[2]Department of Cardiology, The First People's Hospital of Chenzhou, Chenzhou 423000, China
[3]National Clinical Research Center for Geriatric Disorders, Xiangya Hospital, Central South University, Changsha 410008, China

Correspondence to: Chuan-Chang Li; **email:** lichuanchang@csu.edu.cn
Keywords: long non-coding RNA (lncRNA), ANRIL, AMP-activated protein kinase, metformin, atherosclerosis
Received: June 3, 2020 **Accepted:** November 5, 2020 **Published:** December 19, 2020

ABSTRACT

Background: Phenotypic switching of vascular smooth muscle cells (VSMCs) plays a key role in atherosclerosis. Long noncoding RNA ANRIL (lncRNA-ANRIL) is critical in vascular homeostasis. Metformin produces multiple beneficial effects in atherosclerosis. However, the underlying mechanisms need to be elucidated.
Methods and Results: Metformin increased lncRNA-ANRIL expression and AMPK activity in cultured VSMCs, and inhibited the phenotypic switching of VSMCs to the synthetic phenotype induced by platelet-derived growth factor (PDGF). Overexpression of lncRNA-ANRIL inhibited phenotypic switching and reversed the reduction of AMPK activity in PDGF-treated VSMCs. While, gene knockdown of lncRNA-ANRIL by adenovirus or silence of AMPKγ through siRNA abolished AMPK activation induced by metformin in VSMCs. RNA-immunoprecipitation analysis indicated that the affinity of lncRNA-ANRIL to AMPKγ subunit was increased by metformin. *In vivo*, administration of metformin increased the levels of lncRNA-ANRIL, suppressed VSMC phenotypic switching, and prevented the development of atherosclerotic plaque in *Apoe*$^{-/-}$ mice fed with western diet. These protective effects of metformin were abolished by infecting *Apoe*$^{-/-}$ mice with adenovirus expressing lncRNA-ANRIL shRNA. The levels of AMPK phosphorylation, AMPK activity, and lncRNA-ANRIL expression were decreased in human atherosclerotic lesions. Conclusion: Metformin activates AMPK to suppress the formation of atherosclerotic plaque through upregulation of lncRNA-ANRIL.

INTRODUCTION

It is known that atherosclerosis is a chronic inflammation in arterial wall [1, 2]. Vascular smooth muscle cells (VSMCs) can change the phenotype from contractile to synthetic as a response to multiple stimuli in atherosclerosis [3, 4]. Further characterization and better understanding of the underlying signaling could provide a therapeutic target in the prevention of atherosclerosis.

Protein function can be regulated by RNA-protein interaction [5, 6]. Long noncoding RNA (LncRNA) is important to regulate cellular functions including translation, transcription, and cell differentiation [7, 8]. The ANRIL gene encoding a 3.8 kb lncRNA, consisting of 19 exons, is robustly expressed in vascular cells [9]. Human studies showed that lncRNA-ANRIL expression is reduced in coronary artery samples [10–12]. It is also reported that lncRNA-ANRIL regulates endothelial cell and VSMCs functions by transcriptionally upregulating

several genes expressions [13, 14], revealing the critical roles of lncRNA-ANRIL in controlling vascular functions.

AMP-activated protein kinase (AMPK) is composed of α, β, and γ subunits [15]. The α subunit is a catalytic subunit, while β and γ subunits are regulatory subunits [16, 17]. An increased AMP level is able to activate AMPK through allosteric effect to maintain AMPKα phosphorylation within eukaryotic cells [18]. AMPK is also activated by serval drugs such as metformin, which exerts protective effects and affects VSMC phenotypic switching in vascular cells [19–21].

Based on the aforementioned studies, we speculated that, in VSMCs, lncRNA-ANRIL is a regulator of AMPK to inhibit phenotypic switching. The present study was aimed to establish the link between lncRNA-ANRIL and AMPK, and to test whether metformin prevents atherosclerosis through lncRNA-ANRIL/AMPK signaling.

RESULTS

PDGF reduces lncRNA-ANRIL level and increases phenotypic switching in VSMCs

VSMC phenotypic switching is vital in the formation of atherosclerotic plaque [22]. Platelet-derived growth factor (PDGF) can promote VSMCs switching from the contractile phenotype to synthetic phenotype, which contributes to atherosclerosis [23]. We determined the effects of PDGF on lncRNA-ANRIL *DQ485454* transcript expression, which the expression level of the *DQ485454* transcript was >6-fold higher in atherosclerosis plaque than the levels of full-length *NR_003529* transcript or *EU741058* transcript as reported by Hyosuk Cho et al [13]. Phenotypic switching was detected by using IFC staining of α-SMA. LncRNA-ANRIL expression was assayed by real-time PCR. As indicated in Figure 1A, 1B, PDGF decreased α-SMA, KLF4, and myocardin protein levels, compared to vehicle-treated cells. The mRNA levels of contractile phenotypic markers, such as calponin and smoothelin, were also reduced in PDGF-treated cells (Figure 1C). Gene expressions of synthetic phenotypic markers, including osteopontin, collagen I, and collagen III, were upregulated by PDGF. Besides, the mRNA levels of lncRNA-ANRIL were reduced by PDGF in VSMCs (Figure 1D). These data indicate that PDGF induced phenotypic switching of VSMCs, consistent with other reports [24, 25].

Metformin upregulates lncRNA-ANRIL expression and inhibits PDGF-induced phenotypic switching in VSMCs

Metformin has been reported to activate AMPK and is prescribed worldwide as anti-diabetic drug to manage type 2 diabetes [26]. Epidemiological evidence has demonstrated metformin is more likely to reduce cardiovascular event risk [27]. Thus, we determined the effects of metformin on PDGF-induced phenotypic switching in VSMCs. As shown in Figure 1B, 1E, metformin at 1 mM activated AMPK by increasing AMPK phosphorylation at Thr172, which is essential for AMPK activity [28]. As expected, metformin treatment abolished PDGF-induced the reductions of α-SMA, KLF4, and myocardin (Figure 1B). Metformin increased other contractile phenotypic markers (calponin and smoothelin) but decreased synthetic phenotypic markers (osteopontin, collagen I, and collagen III) in PDGF-treated VSMCs (Figure 1C). These data demonstrate that metformin is able to inhibit phenotypic switching of VSMCs. Further, metformin abrogated PDGF-induced reduction of lncRNA-ANRIL expression in VSMCs (Figure 1D).

Overexpression of lncRNA-ANRIL abolishes PDGF-induced phenotypic switching

To investigate the role of lncRNA-ANRIL in PDGF-induced phenotypic switching, we upregulated lncRNA-ANRIL in VSMCs via adenovirus, which PDGF had no effects on exogenous expression of lncRNA-ANRIL (Figure 2A). As depicted in Figure 2B–2G, in PDGF-treated cells, lncRNA-ANRIL overexpression reversed the expressions of contractile phenotypic markers (α-SMA, calponin, and smoothelin), compared with cells infected with adenovirus alone. However, lncRNA-ANRIL gain-function decreased mRNA levels of synthetic phenotypic markers (osteopontin, collagen I, and collagen III) in PDGF-treated VSMCs. These data demonstrate that PDGF via downregulation of lncRNA-ANRIL induces VSMC phenotypic switching.

Gain-function of lncRNA-ANRIL increases AMPK activity in PDGF-treated VSMCs

To test whether AMPK is involved in PDGF-induced VSMC phenotypic switching via lncRNA-ANRIL dysfunction, we next examined AMPK phosphorylation and activity in lncRNA-ANRIL-overexpressed cells. As presented in Figure 2H, 2I, PDGF significantly inactivated AMPK by decreasing AMPK phosphorylation and its activity in cells infected with adenovirus vector alone, but had no effects on AMPK activity and phosphorylation if cells were overexpressed with lncRNA-ANRIL.

Knockdown of lncRNA-ANRIL ablates pharmacological activations of AMPK in cultured VSMCs

To further confirm whether lncRNA-ANRIL is an upstream modulator of AMPK in VSMCs, cells were infected with shRNA to downregulate lncRNA-ANRIL

expression and then treated with metformin. Adenovirus-mediated shRNA expression inhibited lncRNA-ANRIL expression (Figure 3A). As indicated in Figure 3B, 3C, metformin increased both AMPK activity and AMPK phosphorylation in VSMCs infected with adenovirus vector alone. However, metformin failed to activate AMPK if lncRNA-ANRIL was deficient in cells, demonstrating that metformin via lncRNA-ANRIL activates AMPK.

Inhibition of lncRNA-ANRIL reduces the sensitivity of AMPK to AMP in cells

AICAR is an adenosine analog to generate AMP-mimetic action to activate AMPK [16]. We next infected cells with adenovirus containing lncRNA-ANRIL shRNA and then treated with metformin or AICAR, which did not affect the effects of lncRNA-ANRIL shRNA (Figure 3A). As illustrated in Figure 3B, 3C, AICAR or metformin alone increased AMPK phosphorylation at Thr172 and AMPK activity in VSMCs infected with adenovirus vector alone. This is consistent with previous reports [29, 30].

Antisense oligonucleotide targeting lncRNA-ANRIL inhibits the effects of metformin on AMPK activation

To further implicate whether metformin via upregulating lncRNA-ANRIL activates AMPK, we used antisense oligonucleotide of lncRNA-ANRIL to inhibit the function of lncRNA-ANRIL. As shown in Figure 3D, antisense oligonucleotide of lncRNA-ANRIL reversed the effects on metformin in AMPK phosphorylation. We also observed that metformin increased AMPK phosphorylation in cells with overexpressed lncRNA-ANRIL (Figure 3E), demonstrating that metformin activates AMPK through upregulating lncRNA-ANRIL. The roles of lncRNA-ANRIL in PDGF-induced VSMC phenotypic switching were further examined by detecting the combination of

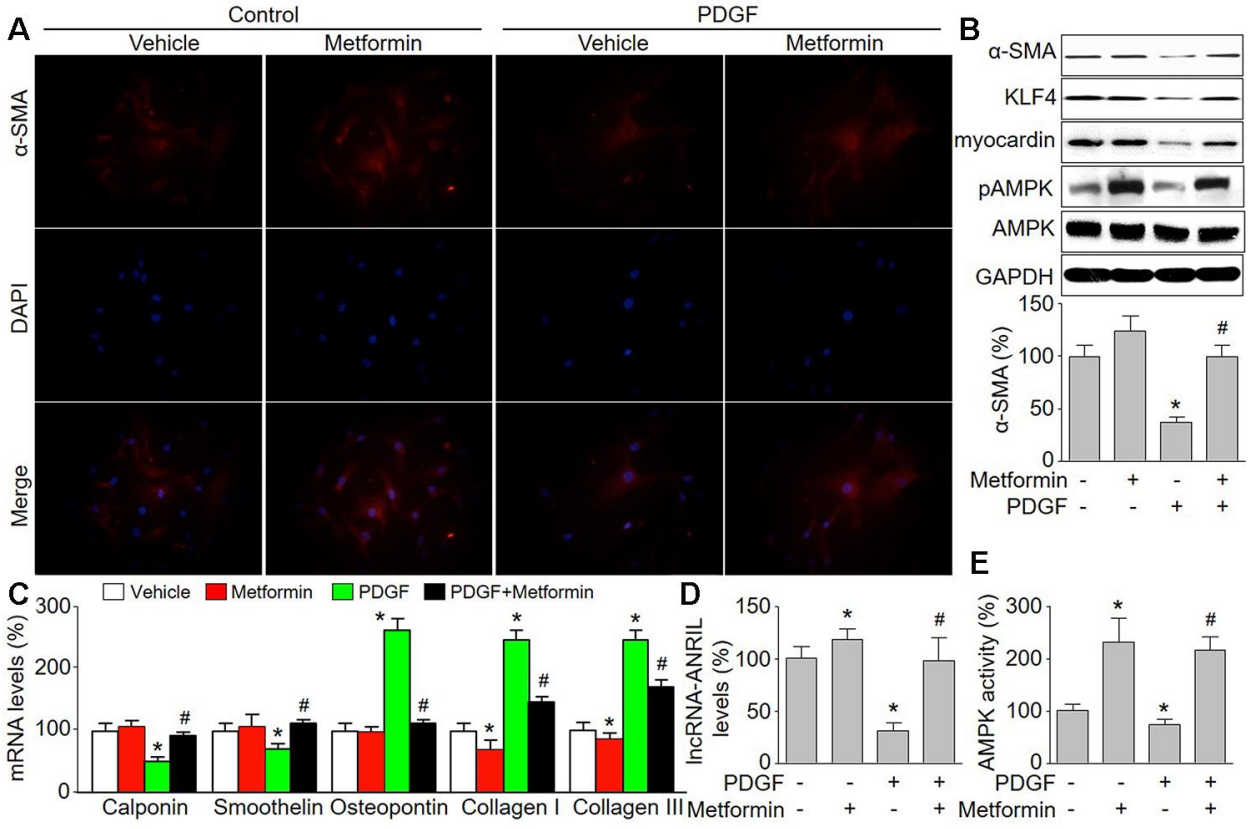

Figure 1. Metformin inhibits PDGF-induced phenotypic switching and increases the expressions of lncRNA-ANRIL in cultured VSMCs. Cultured VSMCs were treated with PDGF (5 ng/ml) for 48 hours in presence or absence of metformin (1 mM). (**A**) The morphology of contractile phenotype in cells was determined by immunofluorescence analysis of alpha SMA (α-SMA). (**B**) Total cell lysates were subjected to perform western blot analysis of phosphorylated AMPK (pAMPK), total AMPK protein levels, α-SMA, KLF4, and myocardin. (**C**) The mRNA levels of the phenotypic switching markers, including calponin, smoothelin, osteopontin, collagen I, and collagen III were measured by real-time PCR. (**D**) The lncRNA-ANRIL level was assessed by real-time PCR. (**E**) AMPK activity was assayed by P^{32}-ATP method. N is 5 in each group. $^{*}P<0.05$ vs. Vehicle. $^{\#}P<0.05$ vs. PDGF.

PDGF and the lncRNA-ANRIL shRNA treatment on smooth muscle markers. As shown in Figure 3F–3I, PDGF not only decreased AMPK phosphorylation, but also altered the expression of α-SMA, calponin, and osteopontin in cells with overexpressed lncRNA-ANRIL shRNA.

Metformin increases the binding of AMPKγ with lncRNA-ANRIL in VSMCs

LncRNAs are associated to a plethora of cellular functions, most of which require the interaction with one or more RNA-binding proteins [31]. We next performed RIP analysis to determine the binding between AMPKγ and lncRNA-ANRIL. In Figure 4A, lncRNA-ANRIL, but not lncRNA-MALAT1, was positively detected in samples from cells following RIP with AMPKγ primary antibody, implying that lncRNA-ANRIL is specific to AMPKγ.

LncRNA-ANRIL increases the formation of AMPKαβγ complex

To address what happens to AMPKγ subunit when it's bound to lncRNA-ANRIL, we detected the binding among AMPKα subunit, β subunit, and γ subunit. As shown in Figure 4B, the interaction among AMPKα, β and γ were much more solid in cells with lncRNA-ANRIL overexpression, compared with adenovirus-infected cells, indicating that lncRNA-ANRIL may increase the formation of AMPKαβγ complex.

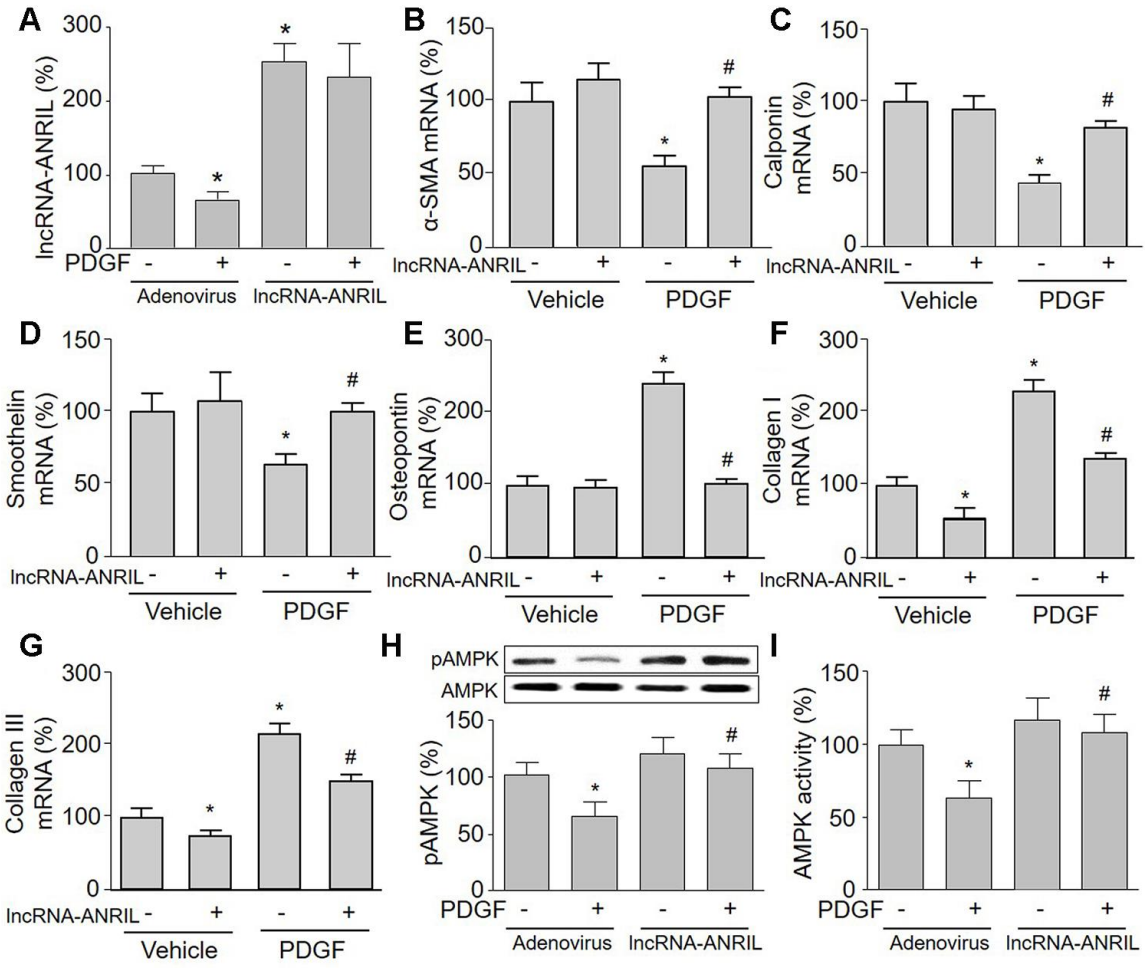

Figure 2. Overexpression of lncRNA-ANRIL abolishes PDGF-induced phenotypic switching and reverses AMPK activity in cultured VSMCs. Cultured VSMCs were infected with adenovirus expressing lncRNA-ANRIL for 24 hours and then treated with PDGF (5 ng/ml) for 48 hours. (**A**) The expression of lncRNA-ANRIL was determined by real-time PCR. N is 5 in each group. $^{*}P<0.05$ vs. adenovirus vector. (**B**–**G**) The mRNA levels of the markers of VSMC phenotypic switching, including α-SMA in B, calponin in C, smoothelin in D, osteopontin in E, collagen I in F, and collagen III in G were measured by real-time PCR. (**H**) Total cell lysates were subjected to perform western blot analysis of phosphorylated AMPK (pAMPK) and total AMPK protein levels. (**I**) AMPK activity was assayed by P^{32}-ATP method. N is 5 in each group. $^{*}P<0.05$ vs. adenovirus alone. $^{\#}P<0.05$ vs. adenovirus + PDGF.

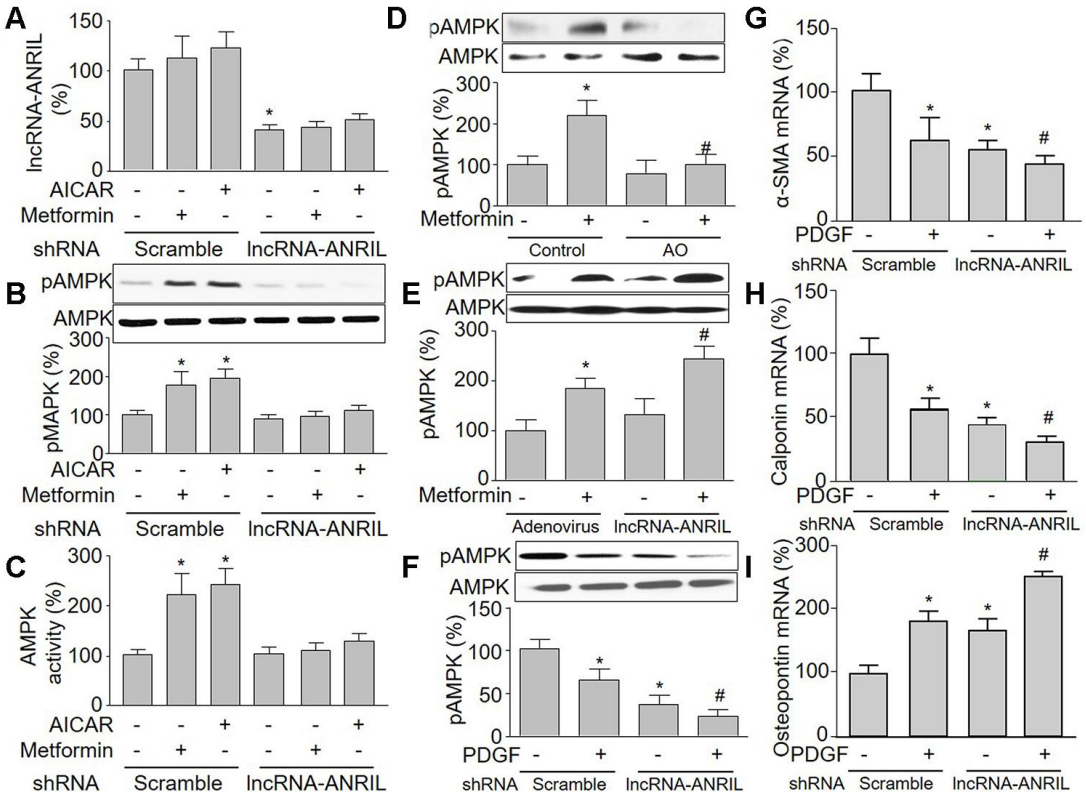

Figure 3. Knockdown of lncRNA-ANRIL ablates pharmacological activations of AMPK in cultured VSMCs. (**A**–**C**) Cultured VSMCs were infected with adenovirus expressing scramble or lncRNA-ANRIL shRNA for 48 hours and then treated with metformin (1 mM) or AICAR (0.5 mM) for 6 hours. (**A**) The expression of lncRNA-ANRIL was determined by real-time PCR. N is 5 in each group. *P<0.05 vs. adenovirus. (**B**) Total cell lysates were subjected to perform western blot analysis of phosphorylated AMPK (pAMPK) and total AMPK protein levels. (**C**) AMPK activity was assayed by P^{32}-ATP method. N is 5 in each group. *P<0.05 vs. scramble shRNA alone. #P<0.05 vs. scramble shRNA plus metformin or AICAR. (**D**) Cultured VSMCs were transfected antisense oligonucleotide of lncRNA-ANRIL (AO) for 48 hours and then treated with metformin (1 mM) for 6 hours. The pAMPK level was assayed by western blot in total cell lysates. N is 5 in each group. *P<0.05 vs. control. #P<0.05 vs. metformin alone. (**E**) Cultured VSMCs were infected with adenovirus expressing lncRNA-ANRIL for 24 hours and then treated with metformin (1 mM) for 6 hours. The pAMPK level was assayed by western blot in total cell lysates. N is 5 in each group. *P<0.05 vs. adenovirus alone. #P<0.05 vs. adenovirus plus metformin. (**F**–**I**) Cultured VSMCs were infected with adenovirus expressing lncRNA-ANRIL shRNA for 24 hours and then treated with PDGF (5 ng/ml) for 48 hours. Total cell lysates were subjected to perform western blot analysis of pAMPK in F. The mRNA levels of the phenotypic switching markers, including α-SMA in (**G**), calponin in (**H**), and osteopontin in I were assessed by real-time PCR. N is 5 in each group. *P<0.05 vs. scramble shRNA alone. #P<0.05 vs. lncRNA-ANRIL shRNA alone.

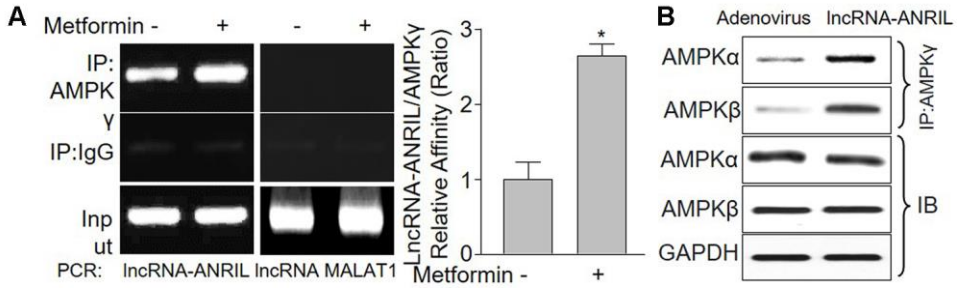

Figure 4. LncRNA-ANRIL regulates AMPK catalytic activity by binding to AMPK gamma subunit. (**A**) Cultured VSMCs were incubated with metformin (1 mM) for 12 hours. Cells were subjected to detect the binding of lncRNA-ANRIL or lncRNA-MALAT1 to AMPKγ subunit by using RNA-immunoprecipitation assay in (**A**) Quantitative analysis of the affinity between lncRNA-ANRIL and AMPKγ was performed. N is 5 in each group. *P<0.05 vs. vehicle. (**B**) Cultured VSMCs were infected with adenovirus expressing lncRNA-ANRIL for 48 hours. The binding of AMPKα or β to AMPKγ was assayed by IP.

Metformin-induced AMPK activation is AMPKγ-dependent in cells

To further verify this concept that metformin activates AMPK through increasing the interaction between lncRNA-ANRIL and AMPKγ, we downregulated AMPKγ subunit via siRNA. As shown in Supplementary Figure 1A, 1B, metformin increased both AMPK phosphorylation and AMPK activity in VSMCs transfected with scramble siRNA, but not in cells transfected with AMPKγ siRNA. Collectively, it indicates that AMPKγ is essential for metformin-induced AMPK activation.

Knockdown of lncRNA-ANRIL ablates the suppressive effects of AMPK activation by metformin on atherosclerotic plaque growth in *Apoe*$^{-/-}$ mice

We further investigated if lncRNA-ANRIL is involved in the growth of atherosclerotic plaque suppressed by metformin *in vivo*. Thus, we infected *Apoe*$^{-/-}$ mice with adenovirus to knockdown lncRNA-ANRIL followed by feeding mice with western diet (Figure 5A). As indicated in Figure 5B, 5D, the size of atherosclerotic plaque was reduced in metformin-treated *Apoe*$^{-/-}$ mice expressing negative control shRNA, compared with vehicle-treated *Apoe*$^{-/-}$ mice expressing scramble shRNA. However, metformin did not decrease atherosclerotic plaque size in *Apoe*$^{-/-}$ mice infected with adenovirus containing lncRNA-ANRIL shRNA. According, metformin increased AMPK activity in atherosclerotic plaque in *Apoe*$^{-/-}$ mice expressing scramble shRNA, but not in *Apoe*$^{-/-}$ mice expressing lncRNA-ANRIL shRNA (Figure 5C). While, the plasms levels of TC, TG, glucose, and plasma cytokine levels were comparable among four groups (Supplementary Tables 2, 3). In sum, it indicates that lncRNA-ANRIL is involved in the effects of metformin in AMPK activation and atherosclerotic plaque growth *in vivo*.

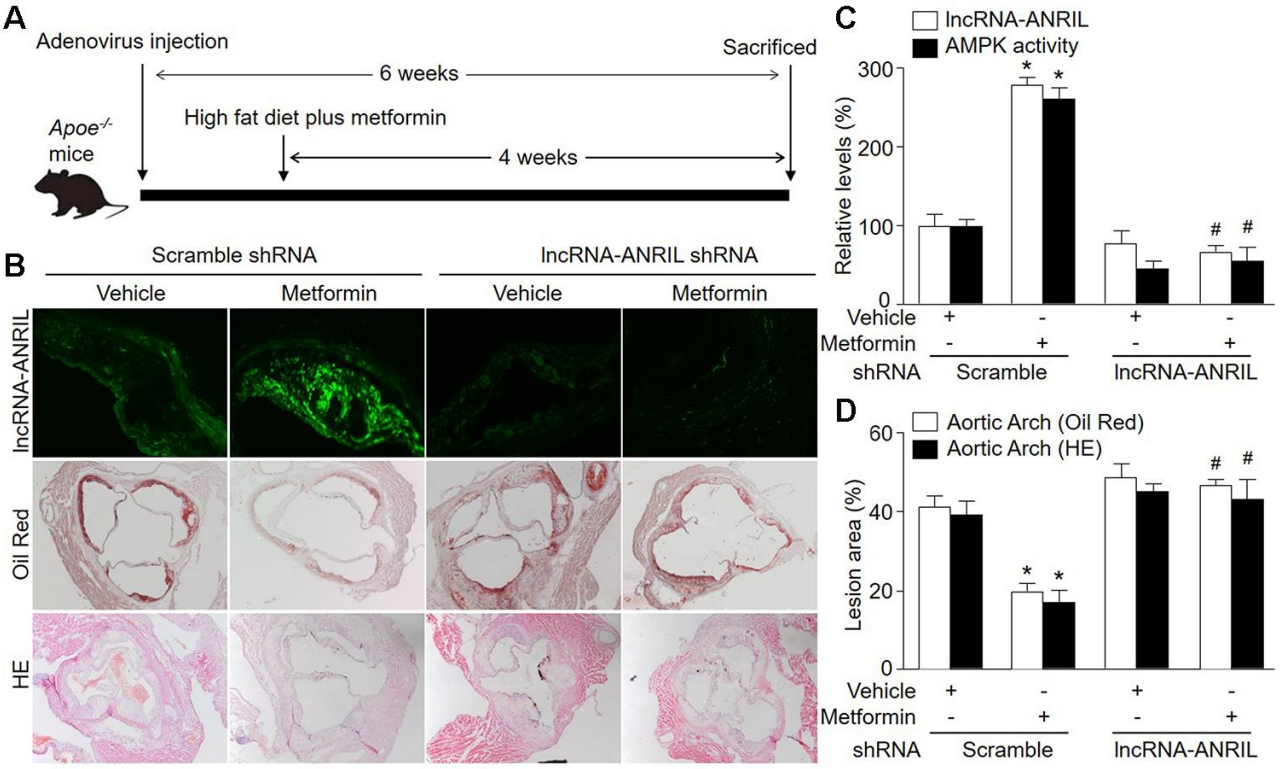

Figure 5. Adenovirus-mediated knockdown of lncRNA-ANRIL prevents the anti-atherosclerotic effects of metformin in *Apoe*$^{-/-}$ mice. (**A**) The protocol of animal experiments in *Apoe*$^{-/-}$ mice. Male *Apoe*$^{-/-}$ mice were injected with adenovirus containing scramble shRNA or lncRNA-ANRIL shRNA to silence lncRNA-ANRIL gene expression. Two weeks later after injection, mice received western diet plus metformin (150 mg/kg/day) in drinking water for 4 weeks. At the end of experiments, all mice were sacrificed under anesthesia. (**B**) The aortic root tissue was subjected to fluorescence in situ hybridization to detect lncRNA-ANRIL expression in green and the morphology analysis of aortic root by Oil Red staining and HE staining. (**C**) The expressional level of lncRNA-ANRIL and AMPK activity in aortic lesion tissue were assayed. (**D**) Quantitative analysis of atherosclerotic lesion size in aortic root by Oil Red staining and HE staining. N is 10-15 in each group. $^{*}P<0.05$ *vs.* scramble shRNA alone. $^{\#}P<0.05$ vs. scramble shRNA plus metformin.

Knockdown of lncRNA-ANRIL abolishes the effects of metformin on VSMC phenotype switching *in vivo*

We next determined whether knockdown of lncRNA-ANRIL could induce VSMC phenotypic switching in atherosclerosis. As shown in Figure 6A, 6B, administration of metformin increased α-SMA content in atherosclerotic plaque in *Apoe*$^{-/-}$ mice fed with western diet infected with adenovirus expressing scramble shRNA. Meanwhile, metformin increased the mRNA levels of other contractile phenotypic markers (calponin and smoothelin) in these *Apoe*$^{-/-}$ mice. Conversely, the expressions of synthetic markers (osteopontin, collagen I, and collagen III) were markedly decreased by metformin in the plaque of *Apoe*$^{-/-}$ mice expressing scramble shRNA. However, metformin treatment had no any effects on the expression of markers including α-SMA, calponin, smoothelin, osteopontin, collagen I, and collagen III in the plaque of *Apoe*$^{-/-}$ mice expressing lncRNA-ANRIL shRNA. Taken together, these results suggest that metformin via lncRNA-ANRIL upregulation suppresses VSMC phenotypic switching in atherosclerosis.

Reduced AMPK phosphorylation, AMPK activity, and lncRNA-ANRIL expression are associated with atherosclerotic lesions in human patients

To establish the clinical association of this study, we determined the level of AMPK activity and AMPK phosphorylation in patients with atherosclerosis. The clinical characters were presented in Supplementary Table 4. As shown in Supplementary Figure 2A, the plaques were seen in atherosclerotic samples (stenosis > 50%). The atherosclerotic tissues exhibited lower levels of AMPK phosphorylation and activity than control samples (Supplementary Figures 2B, 2C). Further, the expression of lncRNA-ANRIL was also decreased in patient with atherosclerosis (Supplementary Figure 2D).

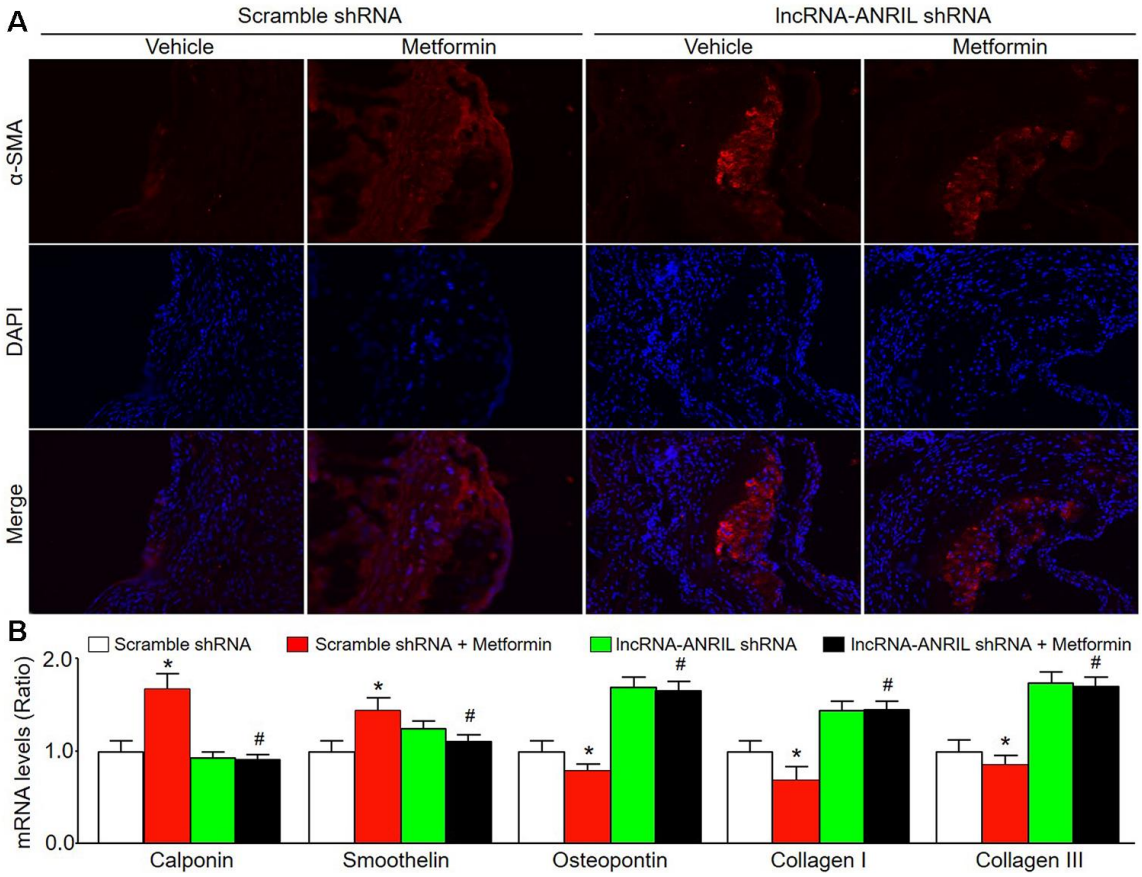

Figure 6. Adenovirus-mediated knockdown of lncRNA-ANRIL prevents the effects of metformin on VSMC phenotype switch in *Apoe*$^{-/-}$ mice. The animal experimental protocol was shown in Figure 5A. (**A**) The morphology of VSMC in atherosclerotic plaque was determined by immunofluorescence analysis of α-SMA. (**B**) The mRNA levels of the markers of VSMC phenotype switch, including calponin, smoothelin, osteopontin, collagen I, and collagen III in aortic tissue were measured by real-time PCR. N is 10-15 in each group. $^{*}P<0.05$ *vs.* scramble shRNA alone. $^{\#}P<0.05$ vs. scramble shRNA plus metformin.

DISCUSSION

In this study, we not only identified lncRNA-ANRIL as an AMPK regulator, but also demonstrated that metformin via lncRNA-ANRIL-dependent AMPK pathway prevents VSMC phenotype switches in the development of atherosclerotic plaque. In cultured cells, metformin upregulates lncRNA-ANRIL expression to increase the interaction between lncRNA-ANRIL and AMPKγ subunit. In mice, AMPK activation by metformin suppressed the growth of atherosclerotic lesion. Importantly, all effects of AMPK activation by metformin were abolished by knockdown of lncRNA-ANRIL via genetic approaches. Thus, we thought that lncRNA-ANRIL upregulation is essential for metformin-suppressed atherosclerosis.

The major discovery of this study is that we identified lncRNA-ANRIL as a novel modulator of AMPK. This is supported by following evidence: (1) The specific binding of AMPKγ to lncRNA-ANRIL was detectable using RIP analysis; (2) LncRNA-ANRIL knockdown decreased metformin-induced AMPK phosphorylation and AMPK activation; (3) The effects of metformin, as a well-recognized AMPK activator, were abolished by lncRNA-ANRIL deficiency *in vitro* and *in vivo.* Although at least two upstream kinases including Calmodulin-dependent kinase kinase (CaMKK) and liver kinase B1 (LKB1) have been identified as AMPK kinases [32, 33], we firstly showed that lncRNA-ANRIL regulates AMPK activity by direct interaction. Linking many functions of AMPK, for example, glucose and lipid metabolisms [34], the finding that lncRNA-ANRIL is an AMPK regulator may expand the applications of lncRNA-ANRIL.

Another important finding is that metformin via lncRNA-ANRIL inhibits VSMC phenotypic switching and the growth of atherosclerotic plaque. Hyosuk Cho et al have identified and validated ten target genes downstream of ANRIL [13]. In this study, we not only identified AMPK as a new target of lncRNA-ANRIL, but also demonstrated that lncRNA-ANRIL/AMPK pathway is critical in the progression of atherosclerosis. Our observations demonstrate that dysregulation of lncRNA-ANRIL in VSMCs affects critical cellular functions by alternating the expressional levels of some key genes of VSMC phenotypic switching.

An issue remained in this study is the signaling pathway by how lncRNA-ANRIL increases APMK activity. Based on our observations, we thought this binding between lncRNA-ANRIL and AMPKγ may increase the stability of AMPKαβγ complex. This wound increase the sensitivity of AMP to AMPK complex and preserve the phosphorylation of AMPKα at Thr172 because we found the formation of AMPKαβγ was increased by lncRNA-ANRIL overexpression and the sensitivity of AICAR to AMPK was also enhanced.

In summary, we identify a novel mechanism by which metformin via lncRNA-ANRIL pathway limits VSMC phenotypic switching, resulting in the suppression of atherosclerosis lesion (Supplementary Figure 3). Because loss of lncRNA-ANRIL can effectively attenuate the effects of AMPK activation, both AMPK and lncRNA-ANRIL might be a therapeutic target on the prevention of atherosclerosis-associated vascular diseases, such as stroke.

MATERIALS AND METHODS

Expanded Materials and Methods are available in Supplementary Material.

Cell culture

As described previously [29], primary murine VSMCs were grown in Smooth Muscle Cell Medium (Sciencell, USA). Cells between passages 4 and 8 were used.

Western blot analysis

Total 20 μg protein were subjected to western blot analysis as described previously [35].

RNA-immunoprecipitation (IP) assay

As described previously [36], lysates were incubated in cold room overnight with magnetic protein A/G beads pretreated with antibody. RNA was extracted from IP complex. The PCR primers for lncRNA-ANRIL are shown in Supplementary Table 1.

Animal experimental protocol

Male *Apoe*$^{-/-}$ mice were obtained from Beijing Huafukang Animal Experimental Center. Mice received tail vein injection of adenovirus. Two weeks after injection, mice were fed with western diet plus metformin (150 mg/kg/day) in drinking water for 4 weeks. At the end of experiments, mice were sacrificed under anesthesia by intraperitoneal injection of 0.8% pentobarbital sodium (60 mg/kg).

Atherosclerotic lesion analysis

As described previously [37], Oil Red staining was used for neutral lipids in atherosclerotic lesion.

AMPK activity assay

The SAMS peptide was used to assay AMPK activity as previously described [38, 39].

Statistical analysis

All data are expressed as mean ± S.E.M. Multiple comparisons were performed using a one-way ANOVA followed by Bonferroni corrections. Two-sided $P < 0.05$ was considered significant.

AUTHOR CONTRIBUTIONS

D.J.H. designed and conducted the experiments, and analyzed data. Z.Y.L and Y.T.Z. partially performed some experiments. C.C.L. designed and performed the experiments, analyzed data, wrote the manuscript, and convinced the whole project.

CONFLICTS OF INTEREST

These authors declare no conflicts of interest.

FUNDING

This work was supported by grants from the National Natural Science Foundation of China (No. 81570461 and No. 81873509) and Natural Science Foundation of Hunan Province (NO. 2018JJ6057).

REFERENCES

1. Ross R. Atherosclerosis—an inflammatory disease. N Engl J Med. 1999; 340:115–26. https://doi.org/10.1056/NEJM199901143400207 PMID:9887164

2. Libby P. Inflammation in atherosclerosis. Nature. 2002; 420:868–74. https://doi.org/10.1038/nature01323 PMID:12490960

3. Chappell J, Harman JL, Narasimhan VM, Yu H, Foote K, Simons BD, Bennett MR, Jørgensen HF. Extensive proliferation of a subset of differentiated, yet plastic, medial vascular smooth muscle cells contributes to neointimal formation in mouse injury and atherosclerosis models. Circ Res. 2016; 119:1313–23. https://doi.org/10.1161/CIRCRESAHA.116.309799 PMID:27682618

4. Shankman LS, Gomez D, Cherepanova OA, Salmon M, Alencar GF, Haskins RM, Swiatlowska P, Newman AA, Greene ES, Straub AC, Isakson B, Randolph GJ, Owens GK. KLF4-dependent phenotypic modulation of smooth muscle cells has a key role in atherosclerotic plaque pathogenesis. Nat Med. 2015; 21:628–37. https://doi.org/10.1038/nm.3866 PMID:25985364

5. Zhou SN, Lu JX, Wang XQ, Shan MR, Miao Z, Pan GP, Jian X, Li P, Ping S, Pang XY, Bai YP, Liu C, Wang SX. S-nitrosylation of prostacyclin synthase instigates nitrate cross-tolerance in vivo. Clin Pharmacol Ther. 2019; 105:201–09. https://doi.org/10.1002/cpt.1094 PMID:29672839

6. Licatalosi DD, Darnell RB. RNA processing and its regulation: global insights into biological networks. Nat Rev Genet. 2010; 11:75–87. https://doi.org/10.1038/nrg2673 PMID:20019688

7. Ferrè F, Colantoni A, Helmer-Citterich M. Revealing protein-lncRNA interaction. Brief Bioinform. 2016; 17:106–16. https://doi.org/10.1093/bib/bbv031 PMID:26041786

8. Bai YP, Zhang JX, Sun Q, Zhou JP, Luo JM, He LF, Lin XC, Zhu LP, Wu WZ, Wang ZY, Zhang GG. Induction of microRNA-199 by nitric oxide in endothelial cells is required for nitrovasodilator resistance via targeting of prostaglandin I2 synthase. Circulation. 2018; 138:397–411. https://doi.org/10.1161/CIRCULATIONAHA.117.029206 PMID:29431644

9. Holdt LM, Hoffmann S, Sass K, Langenberger D, Scholz M, Krohn K, Finstermeier K, Stahringer A, Wilfert W, Beutner F, Gielen S, Schuler G, Gäbel G, et al. Alu elements in ANRIL non-coding RNA at chromosome 9p21 modulate atherogenic cell functions through trans-regulation of gene networks. PLoS Genet. 2013; 9:e1003588. https://doi.org/10.1371/journal.pgen.1003588 PMID:23861667

10. Holdt LM, Teupser D. Recent studies of the human chromosome 9p21 locus, which is associated with atherosclerosis in human populations. Arterioscler Thromb Vasc Biol. 2012; 32:196–206. https://doi.org/10.1161/ATVBAHA.111.232678 PMID:22258902

11. Wang F, Xu CQ, He Q, Cai JP, Li XC, Wang D, Xiong X, Liao YH, Zeng QT, Yang YZ, Cheng X, Li C, Yang R, et al. Genome-wide association identifies a susceptibility locus for coronary artery disease in the Chinese Han population. Nat Genet. 2011; 43:345–49. https://doi.org/10.1038/ng.783 PMID:21378986

12. McPherson R, Pertsemlidis A, Kavaslar N, Stewart A, Roberts R, Cox DR, Hinds DA, Pennacchio LA, Tybjaerg-Hansen A, Folsom AR, Boerwinkle E, Hobbs HH, Cohen JC. A common allele on chromosome 9 associated with coronary heart disease. Science. 2007; 316:1488–91. https://doi.org/10.1126/science.1142447 PMID:17478681

13. Cho H, Shen GQ, Wang X, Wang F, Archacki S, Li Y, Yu G, Chakrabarti S, Chen Q, Wang QK. Long noncoding RNA ANRIL regulates endothelial cell activities associated with coronary artery disease by up-regulating CLIP1, EZR, and LYVE1 genes. J Biol Chem. 2019; 294:3881–98. https://doi.org/10.1074/jbc.RA118.005050 PMID:30655286

14. Lo Sardo V, Chubukov P, Ferguson W, Kumar A, Teng EL, Duran M, Zhang L, Cost G, Engler AJ, Urnov F, Topol EJ, Torkamani A, Baldwin KK. Unveiling the role of the most impactful cardiovascular risk locus through haplotype editing. Cell. 2018; 175:1796–810.e20. https://doi.org/10.1016/j.cell.2018.11.014 PMID:30528432

15. Wang S, Zhang M, Liang B, Xu J, Xie Z, Liu C, Viollet B, Yan D, Zou MH. AMPKalpha2 deletion causes aberrant expression and activation of NAD(P)H oxidase and consequent endothelial dysfunction in vivo: role of 26S proteasomes. Circ Res. 2010; 106:1117–28. https://doi.org/10.1161/CIRCRESAHA.109.212530 PMID:20167927

16. Kim J, Yang G, Kim Y, Kim J, Ha J. AMPK activators: mechanisms of action and physiological activities. Exp Mol Med. 2016; 48:e224. https://doi.org/10.1038/emm.2016.16 PMID:27034026

17. Wang S, Zhang C, Zhang M, Liang B, Zhu H, Lee J, Viollet B, Xia L, Zhang Y, Zou MH. Activation of AMP-activated protein kinase α2 by nicotine instigates formation of abdominal aortic aneurysms in mice in vivo. Nat Med. 2012; 18:902–10. https://doi.org/10.1038/nm.2711 PMID:22561688

18. Liang WJ, Zhou SN, Shan MR, Wang XQ, Zhang M, Chen Y, Zhang Y, Wang SX, Guo T. AMPKα inactivation destabilizes atherosclerotic plaque in streptozotocin-induced diabetic mice through AP-2α/miRNA-124 axis. J Mol Med (Berl). 2018; 96:403–12. https://doi.org/10.1007/s00109-018-1627-8 PMID:29502204

19. Vasamsetti SB, Karnewar S, Kanugula AK, Thatipalli AR, Kumar JM, Kotamraju S. Metformin inhibits monocyte-to-macrophage differentiation via AMPK-mediated inhibition of STAT3 activation: potential role in atherosclerosis. Diabetes. 2015; 64:2028–41. https://doi.org/10.2337/db14-1225 PMID:25552600

20. Gopoju R, Panangipalli S, Kotamraju S. Metformin treatment prevents SREBP2-mediated cholesterol uptake and improves lipid homeostasis during oxidative stress-induced atherosclerosis. Free Radic Biol Med. 2018; 118:85–97. https://doi.org/10.1016/j.freeradbiomed.2018.02.031 PMID:29499335

21. Ding Y, Zhang M, Zhang W, Lu Q, Cai Z, Song P, Okon IS, Xiao L, Zou MH. AMP-activated protein kinase alpha 2 deletion induces VSMC phenotypic switching and reduces features of atherosclerotic plaque stability. Circ Res. 2016; 119:718–30. https://doi.org/10.1161/CIRCRESAHA.116.308689 PMID:27439892

22. Lin H, Ni T, Zhang J, Meng L, Gao F, Pan S, Luo H, Xu F, Ru G, Chi J, Guo H. Knockdown of Herp alleviates hyperhomocysteinemia mediated atherosclerosis through the inhibition of vascular smooth muscle cell phenotype switching. Int J Cardiol. 2018; 269:242–49. https://doi.org/10.1016/j.ijcard.2018.07.043 PMID:30017525

23. Wang TM, Chen KC, Hsu PY, Lin HF, Wang YS, Chen CY, Liao YC, Juo SH. microRNA let-7g suppresses PDGF-induced conversion of vascular smooth muscle cell into the synthetic phenotype. J Cell Mol Med. 2017; 21:3592–601. https://doi.org/10.1111/jcmm.13269 PMID:28699690

24. Zeng Z, Xia L, Fan X, Ostriker AC, Yarovinsky T, Su M, Zhang Y, Peng X, Xie Y, Pi L, Gu X, Chung SK, Martin KA, et al. Platelet-derived miR-223 promotes a phenotypic switch in arterial injury repair. J Clin Invest. 2019; 129:1372–86. https://doi.org/10.1172/JCI124508 PMID:30645204

25. Yuan X, Zhang T, Yao F, Liao Y, Liu F, Ren Z, Han L, Diao L, Li Y, Zhou B, He F, Wang L. THO complex-dependent posttranscriptional control contributes to vascular smooth muscle cell fate decision. Circ Res. 2018; 123:538–49. https://doi.org/10.1161/CIRCRESAHA.118.313527 PMID:30026254

26. Hunter RW, Hughey CC, Lantier L, Sundelin EI, Peggie M, Zeqiraj E, Sicheri F, Jessen N, Wasserman DH, Sakamoto K. Metformin reduces liver glucose production by inhibition of fructose-1-6-bisphosphatase. Nat Med. 2018; 24:1395–406. https://doi.org/10.1038/s41591-018-0159-7 PMID:30150719

27. Griffin SJ, Leaver JK, Irving GJ. Impact of metformin on cardiovascular disease: a meta-analysis of randomised trials among people with type 2 diabetes. Diabetologia. 2017; 60:1620–29. https://doi.org/10.1007/s00125-017-4337-9 PMID:28770324

28. Hawley SA, Davison M, Woods A, Davies SP, Beri RK, Carling D, Hardie DG. Characterization of the AMP-activated protein kinase kinase from rat liver and identification of threonine 172 as the major site at which it phosphorylates AMP-activated protein kinase. J Biol Chem. 1996; 271:27879–87.

https://doi.org/10.1074/jbc.271.44.27879 PMID:8910387

29. Wang S, Liang B, Viollet B, Zou MH. Inhibition of the AMP-activated protein kinase-α2 accentuates agonist-induced vascular smooth muscle contraction and high blood pressure in mice. Hypertension. 2011; 57:1010–17. https://doi.org/10.1161/HYPERTENSIONAHA.110.168906 PMID:21464390

30. Wang S, Xu J, Song P, Viollet B, Zou MH. In vivo activation of AMP-activated protein kinase attenuates diabetes-enhanced degradation of GTP cyclohydrolase I. Diabetes. 2009; 58:1893–901. https://doi.org/10.2337/db09-0267 PMID:19528375

31. Zhu J, Fu H, Wu Y, Zheng X. Function of lncRNAs and approaches to lncRNA-protein interactions. Sci China Life Sci. 2013; 56:876–85. https://doi.org/10.1007/s11427-013-4553-6 PMID:24091684

32. Shaw RJ, Kosmatka M, Bardeesy N, Hurley RL, Witters LA, DePinho RA, Cantley LC. The tumor suppressor LKB1 kinase directly activates AMP-activated kinase and regulates apoptosis in response to energy stress. Proc Natl Acad Sci USA. 2004; 101:3329–35. https://doi.org/10.1073/pnas.0308061100 PMID:14985505

33. Hawley SA, Pan DA, Mustard KJ, Ross L, Bain J, Edelman AM, Frenguelli BG, Hardie DG. Calmodulin-dependent protein kinase kinase-beta is an alternative upstream kinase for AMP-activated protein kinase. Cell Metab. 2005; 2:9–19. https://doi.org/10.1016/j.cmet.2005.05.009 PMID:16054095

34. Steinberg GR, Kemp BE. AMPK in health and disease. Physiol Rev. 2009; 89:1025–78. https://doi.org/10.1152/physrev.00011.2008 PMID:19584320

35. Zhang HM, Liu MY, Lu JX, Zhu ML, Jin Q, Ping S, Li P, Jian X, Han YL, Wang SX, Li XY. Intracellular acidosis via activation of Akt-Girdin signaling promotes post ischemic angiogenesis during hyperglycemia. Int J Cardiol. 2019; 277:205–11. https://doi.org/10.1016/j.ijcard.2018.08.028 PMID:30316647

36. Bierhoff H. Analysis of lncRNA-protein interactions by RNA-protein pull-down assays and RNA immunoprecipitation (RIP). Methods Mol Biol. 2018; 1686:241–50. https://doi.org/10.1007/978-1-4939-7371-2_17 PMID:29030825

37. Yang JJ, Li P, Wang F, Liang WJ, Ma H, Chen Y, Ma ZM, Li QZ, Peng QS, Zhang Y, Wang SX. Activation of activator protein 2 alpha by aspirin alleviates atherosclerotic plaque growth and instability in vivo. Oncotarget. 2016; 7:52729–39. https://doi.org/10.18632/oncotarget.10400 PMID:27391154

38. Witters LA, Kemp BE. Insulin activation of acetyl-CoA carboxylase accompanied by inhibition of the 5'-AMP-activated protein kinase. J Biol Chem. 1992; 267:2864–67. PMID:1346611

39. Zhang M, Zhu H, Ding Y, Liu Z, Cai Z, Zou MH. AMP-activated protein kinase α1 promotes atherogenesis by increasing monocyte-to-macrophage differentiation. J Biol Chem. 2017; 292:7888–903. https://doi.org/10.1074/jbc.M117.779447 PMID:28330873

SUPPLEMENTARY MATERIALS

Supplementary Materials and Methods

Reagents and animals

Polyclonal or monoclonal antibodies against pAMPKα-Thr172, AMPKα, AMPKγ1, and α-SMA were obtained from Santa Cruz Biotechnology or Cell Signaling Company. All secondary antibodies were from Cell Signaling Technology. AMPKγ1 siRNA was from Santa Cruz. All PCR primers were purchased from Invitrogen. Other chemicals, if not indicated, were from Sigma-Aldrich (St. Louis, MO). Male *Apoe*$^{-/-}$ mice were obtained from Beijing Huafukang Animal Experimental Center. Mice were housed in temperature-controlled cages with a 12-hrs light-dark cycle. The animal protocol was reviewed and approved by the University of Central South Animal Care and Use Committee.

Cell culture

Primary murine vascular smooth muscle cells (VSMCs) isolated from mice were grown in Smooth Muscle Cell Medium (Sciencell, USA) supplemented with 2% fetal bovine serum, penicillin (100U/ml) and streptomycin (10mg/ml) as described previously [1]. In all experiments, cells were used between passages 4 and 8. All cells were incubated at 37° C in a humidified atmosphere of 5% CO_2 and 95% air. Cells were grown to 80% confluency before being treated with different agents.

Transfection of siRNA into cells

Transient transfection of siRNA was carried out according to Santa Cruz's protocol [2]. Briefly, the siRNAs were dissolved in siRNA buffer (20 mM KCl; 6 mM HEPES, pH 7.5; 0.2 mM $MgCl_2$) to prepare a 10 μM stock solution. Cells grown in 6 well plates were transfected with siRNA in transfection medium (Gibcol) containing liposomal transfection reagent (Lipofectamine RNAimax, Invitrogen). For each transfection, 100 μl transfection medium containing 4 μl siRNA stock solution was gently mixed with 100 μl transfection medium containing 4 μl transfection reagent. After 30-min incubation at room temperature, siRNA-lipid complexes were added to the cells in 1.0 ml transfection medium, and cells were incubated with this mixture for 6 h at 37° C. The transfection medium was then replaced with normal medium, and cells were cultured for 48 hours.

Generations of DNA constructs

LncRNA-ANRIL cDNA or shRNA was purchased from Origene Company. The adenovirus construction compassing lncRNA-ANRIL cDNA or shRNA was generated using the AdMax (Microbix) and pSilencer™ adeno 1.0-CMV (Ambion) systems according to the manufacturers' recommendations. Viruses were packaged and amplified in HEK293A cells and purified using $CsCl_2$ banding followed by dialysis against 10 mM Tris-buffered saline with 10% glycerol. Titering was performed on HEK293 cells using the Adeno-X Rapid Titer kit (BD Biosciences Clontech, Palo Alto, CA, USA) according to the manufacturer's instructions.

Adenovirus infections to cells or animals

Cells were infected with adenovirus overnight in antibiotics-free medium supplemented with 2% FBS. The cells were then washed and incubated in fresh medium for an additional 12-hour before experiments. For infecting mice, adenovirus was injected via tail vein under pressure in 100μl of PBS with 7.6 X 10^7 IFUs of loaded virus. The concentration of DNA was 10 mg/kg.

Western blot analysis

Cell lysates or tissue homogenates were subjected to western blot analysis, as described previously [3]. The protein content was assayed by BCA protein assay reagent (Pierce, USA). Protein of 20 μg was loaded to SDS-PAGE and then transferred to membrane. Membrane was incubated with a 1:1000 dilution of primary antibody, followed by a 1:5000 dilution of horseradish peroxidase-conjugated secondary antibody. Protein bands were visualized by ECL (GE Healthcare). The intensity (area X density) of the individual bands on Western blots was measured by densitometry (model GS-700, Imaging Densitometer; Bio-Rad).

RNA-immunoprecipitation (IP) assay

The Magna RIP kit was used for RNA IP assay as described previously [4]. Briefly, whole-cell lysates were incubated at 4° C overnight with magnetic protein A/G beads pretreated with 5 μg rabbit IgG or AMPK gamma antibody. Beads were washed and incubated with proteinase K buffer (30 min at 55° C), then RNA was isolated from immunoprecipitates, and cDNA was synthesized. lncRNA-ANRIL cDNA was amplified by PCR.

RNA quantifications by RT-qPCR

Total RNA was isolated using a TRIzol-based (Invitrogen) RNA isolation protocol. For mRNA detections, the iScript cDNA Synthesis Kit (Bio-Rad) was used to synthesize first-strand cDNA according to

the manufacturer's protocol [5]. Reactions were run for 30 cycles at conditions as follows: denaturation for 30 seconds at 94° C, annealing for 30 seconds at 57° C, and extension for 30 seconds at 72° C. Constitutively expressed GADPH mRNA was amplified as control. All primers were presented in supplementary Table 1.

Animal experimental protocols

Mice received tail vein injection of adenovirus containing scramble shRNA or lncRNA-ANRIL shRNA. Two weeks later after injection, mice were received western diet with or without metformin (150 mg/kg/day) in drinking water for 4 weeks. At the end of experiments, all mice were sacrificed under anesthesia by intraperitoneal injection of 0.8% pentobarbital sodium (60 mg/kg).

Atherosclerotic lesion analysis

As described previously [6], after being fed the Western diet for 4 weeks, the mice were fasted for 14 h and then were anesthetized and euthanized. The heart and aortic tissue were removed from the ascending aorta to the ileal bifurcation and placed in 4% paraformaldehyde for 16 h. After fixation, the adventitia was thoroughly cleaned under a dissecting microscope. For analyzing the lesion area in the aortic root, the heart was dissected from the aorta, embedded in Polyfreeze tissue freezing medium (Polysciences, Inc) and sectioned (5 μm thickness). Four consecutive sections were collected from each mouse and stained with Oil Red O for neutral lipids, and counterstained with hematoxylin to visualize the nuclei. Plaques were captured under the Olympus microscope connected to a QImaging Retiga CCD camera. The aortic lesion size of each animal was obtained by the averaging of lesion areas in four sections from the same mouse. Digital images of the aorta were captured under a stereomicroscopy, and the lesion area was quantified from the aortic arch to 5 mm distal of the left subclavian artery using Alpha Ease FC software (version 4.0 Alpha Innotech).

Immunofluorescence (IFC)

As described previously [7], after treatment, cells on sterile glass cover slips were rinsed by cold PBS and then fixed by incubation with 10% formalin in PBS for 10 minutes. Block cells by 5% BSA for 30 minutes. Incubate cells with primary antibody for 1 hour at room temperature or overnight at 4° C. After washing, incubate with fluorescence-conjugated secondary antibody for 45 minutes. Take picture in fluorescence microscope.

Detection of lncRNA-ANRIL by fluorescence in situ hybridization (FISH)

As described previously with minor modifications [5], FISH of lncRNA-ANRIL was performed on 5-μm paraffin embedded arterial sections. Briefly, paraffin embedded tissue sections were cut using a microtome (Leica, RM2235) and mounted on polylysine microscope slides (Fisher Scientific) and stored at room temperature (RT) until FISH. Paraffin wax was removed in xylene, sections rehydrated in a series of decreasing ethanol solutions and washed with PBS before fixing in 4% paraformaldehyde. To block endogenous peroxide activity, tissue sections were treated with 0.3% H_2O_2 and washed in PBS before acetylating in acetic anhydride/triethanolamine. Sections were then washed in 2 X SSC and PBS before permeabilization with proteinase K (5 μg/ml) and washes with PBS. Probes (5' and 3'-DIG labelled LNA miRCURY probes; Exiqon) were denatured at 90° C before dilution in hybridization buffer (50% formamide, 0.3 M NaCl, 20 mM Tris-HCL, 5 mM EDTA, 10 mM $NaPO_4$, 10% Dextran sulphate, 1 X Denhardt's solution, 0.5 mg/ml yeast tRNA). Tissue sections were hybridized with lncRNA-ANRIL (200 nM) overnight at 21° C below the predicted Tm value of the probe. After post-hybridization washes in 5 X SSC at RT; 50% formamide/1 X SSC/0.1% Tween 20 at the hybridization temperature; 0.2 X SSC at RT, FISH signals were detected using an Anti-Digoxigenin antibody and the tyramide signal amplification system (PerkinElmer) according to the manufacturer's instructions. Tissue sections were mounted in Vectashield (Vector laboratories). All fluorescence images were analyzed with a Nikon TE2000-U inverted microscope.

AMPK activity assay

AMPK activity was assayed by using the SAMS peptide as previously described [8]. Briefly, duplicate tubes with 200 μg of protein from each sample were prepared and mixed with 500 μl of IP buffer (lysis buffer plus 1 mM dithiothreitol). AMPK was then immunoprecipitated by adding 10 μg of polyclonal antibody against AMPK and 25 μl of Protein A/G-agarose and incubated at 4° C. After centrifugation (14,000 *g*, 1 min), the beads were washed with IP buffer and then twice with 10X reaction buffer (400 mM HEPES, pH 7.4, 800 mM NaCl, 50 mM $MgCl_2$, 1 mM dithiothreitol). The AMPK activity was assayed by adding 50 μl of reaction mixtures, consisting of 5 μl of reaction buffer, 10 μl of SAMS peptide (1 mg/ml), 10 μl of ATP working stock consisting of 0.1 μl of 100 mM ATP, 1 μl of ^{32}P-ATP, and 8.9 μl of H_2O, 25 μl H_2O, or 25 μl of 400 μM AMP, and incubated at 37° C for 10 min. The beads were quickly pelleted, and 25 μl of supernatant was spotted onto P81 Whatman paper. The

filter papers were then washed four or five times with 1% phosphoric acid. After the final wash, the filters were quickly dried and counted in a scintillation counter. The difference between the presence and absence of AMPK is calculated as the AMPK activity.

Measurements of blood glucose, cholesterol, triglyceride, and plasma cytokine levels

The determinations of blood glucose, cholesterol, triglyceride, and plasma cytokine levels in serum were assayed using commercial kits, which were accordance with the protocols as described previously [7].

Patients and sample processing

Left anterior descending coronary arteries were obtained from human subjects after sudden death. The demographic data were presented in Supplementary Table 3. The histology of left anterior descending coronary artery was determined by HE staining. Atherosclerosis was diagnosed as the amount of stenosis of lumen was over 100%. The study was conducted in accordance with the principles of Good Clinical Practice and the Declaration of Helsinki. The study protocol was approved by the Ethical Committee of Central South University Xiangya Hospital, and informed consent was obtained from each human subject.

Statistical analysis

All quantitative results are expressed as mean ± SEM. The normal distribution of data was tested by the Kolmogorov-Smirnov test before statistical comparisons, and the normality/equal variance was tested to determine whether ANOVA was appropriate. All data were analyzed with a 1-way ANOVA followed by Bonferroni *post-hoc* analyses. Comparisons between two groups were analyzed by unpaired Student's *t* test between two groups. Statistical analysis was conducted using IBM SPSS statistics 20.0 (IBM Corp., Armonk, NY, USA), and a two-sided *P*-value < 0.05 was considered significant.

REFERENCES

1. Wang S, Zhang C, Zhang M, Liang B, Zhu H, Lee J, Viollet B, Xia L, Zhang Y, Zou MH. Activation of AMP-activated protein kinase α2 by nicotine instigates formation of abdominal aortic aneurysms in mice in vivo. Nat Med. 2012; 18:902–10. https://doi.org/10.1038/nm.2711 PMID:22561688

2. Wang S, Xu J, Song P, Wu Y, Zhang J, Chul Choi H, Zou MH. Acute inhibition of guanosine triphosphate cyclohydrolase 1 uncouples endothelial nitric oxide synthase and elevates blood pressure. Hypertension. 2008; 52:484–90. https://doi.org/10.1161/HYPERTENSIONAHA.108.112094 PMID:18645049

3. Wang S, Xu J, Song P, Viollet B, Zou MH. In vivo activation of AMP-activated protein kinase attenuates diabetes-enhanced degradation of GTP cyclohydrolase I. Diabetes. 2009; 58:1893–901. https://doi.org/10.2337/db09-0267 PMID:19528375

4. Li J, Gong L, Liu S, Zhang Y, Zhang C, Tian M, Lu H, Bu P, Yang J, Ouyang C, Jiang X, Wu J, Zhang Y, et al. Adipose HuR protects against diet-induced obesity and insulin resistance. Nat Commun. 2019; 10:2375. https://doi.org/10.1038/s41467-019-10348-0 PMID:31147543

5. Bai YP, Zhang JX, Sun Q, Zhou JP, Luo JM, He LF, Lin XC, Zhu LP, Wu WZ, Wang ZY, Zhang GG. Induction of microRNA-199 by nitric oxide in endothelial cells is required for nitrovasodilator resistance via targeting of prostaglandin I2 synthase. Circulation. 2018; 138:397–411. https://doi.org/10.1161/CIRCULATIONAHA.117.029206 PMID:29431644

6. Ding Y, Zhang M, Zhang W, Lu Q, Cai Z, Song P, Okon IS, Xiao L, Zou MH. AMP-activated protein kinase alpha 2 deletion induces VSMC phenotypic switching and reduces features of atherosclerotic plaque stability. Circ Res. 2016; 119:718–30. https://doi.org/10.1161/CIRCRESAHA.116.308689 PMID:27439892

7. Li P, Yin YL, Guo T, Sun XY, Ma H, Zhu ML, Zhao FR, Xu P, Chen Y, Wan GR, Jiang F, Peng QS, Liu C, et al. Inhibition of aberrant MicroRNA-133a expression in endothelial cells by statin prevents endothelial dysfunction by targeting GTP cyclohydrolase 1 in vivo. Circulation. 2016; 134:1752–65. https://doi.org/10.1161/CIRCULATIONAHA.116.017949 PMID:27765794

8. Wang S, Liang B, Viollet B, Zou MH. Inhibition of the AMP-activated protein kinase-α2 accentuates agonist-induced vascular smooth muscle contraction and high blood pressure in mice. Hypertension. 2011; 57:1010–17. https://doi.org/10.1161/HYPERTENSIONAHA.110.168906 PMID:21464390

Supplementary Figures

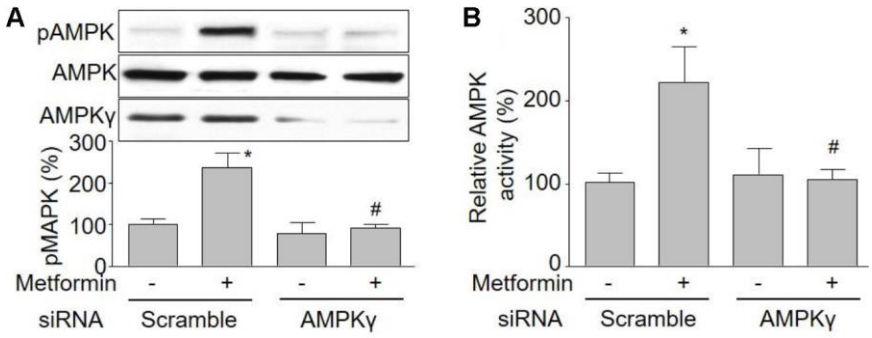

Supplementary Figure 1. LncRNA-ANRIL regulates AMPK catalytic activity by AMPK gamma subunit. Cultured VSMCs were transfected with AMPKγ1 siRNA for 48 hours followed by treatment with metformin (1 mM) for 12 hours. Total cell lysates were subjected to perform western blot analysis of phosphorylated AMPK (pAMPK) and total AMPK protein levels in (**A**). AMPK activity was assayed by P^{32}-ATP method in (**B**). N is 5 in each group. $^{*}P<0.05$ vs. scramble siRNA. $^{\#}P<0.05$ vs. scramble siRNA plus metformin.

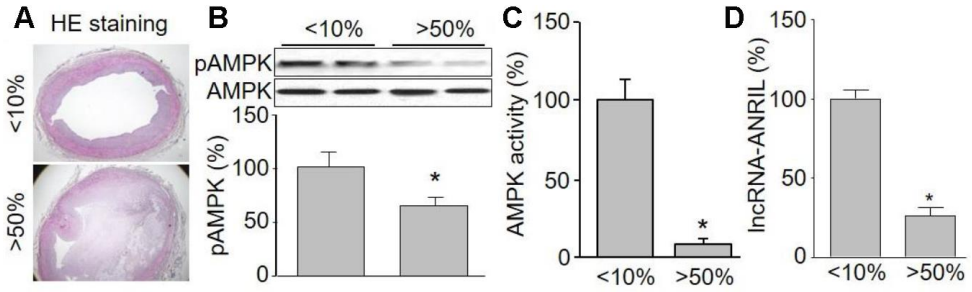

Supplementary Figure 2. Decreased AMPKα phosphorylation and AMPK activity is related to the development of atherosclerosis lesions in human subjects. Tissues of left anterior descending coronary artery were collected from patients with atherosclerosis diagnosed by coronary angiography. (**A**) Morphology of atherosclerosis lesion by HE staining (X100) and IHC analysis of pAMPK and AMPK (X400). (**B**) Quantitative data for pAMPK in A. (**C**) The homogenates of atherosclerotic tissues were subjected to assay the level of pAP-2α by Western blot. (**D**) The lncRNA-ANRIL level was assessed by real-time PCR. Five human subjects in each group. *P<0.05 vs. 10%.

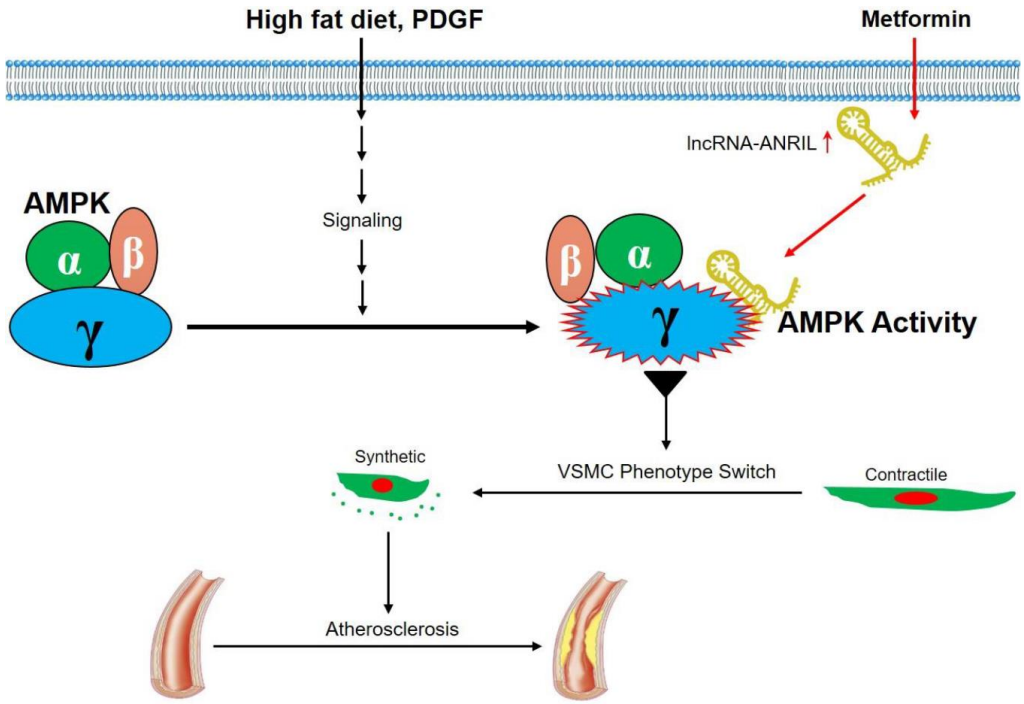

Supplementary Figure 3. Proposed mechanisms by which metformin prevents atherosclerosis. AMPK activation by metformin increases lncRNA-ANRIL expression, leading to the increased affinity of lncRNA-ANRIL to AMPKγ subunit. As a result, AMPK catalytic activity is increased. In this way, metformin produces the suppressive effects on the development of atherosclerosis through suppression of VSMC phenotypic switching.

Supplementary Tables

Supplementary Table 1. Primers used in this project.

Gene	Forward primer sequence (5' - 3')	Reverse primer sequence (5' - 3')
Calponin	GGCAACCAACCACAAATTAGCA	CCCTGCATGCGGTGGAAAAGGC
Smoothelin	GGGGCTCTTGGGAACTACAC	GCCATGAATGTCCACTGTGC
α-SMA	AATGCCACCTTTTGACAGTGATG	TGGAATGTCAAGTCTGCACCA
Collagen I	TGCTTGAGGTGGTTGTGGAA	CAGCAACTGTGACCTGGAGA
Collagen I	CTGATGATCGACCGTGAGAA	GAAGGGTTGGTTCTTTCGAA
Osteopontin	AACTTGGGTTTCAGCACCAC	TACCAGTCCCACGATGTCAG
lncRNA-ANRIL	GTCACTGCAGCTCTGAATGTTTCTT	CCCAGTTGTGCATCGACCTA
GAPDH	AGCTAAGAGAAGGGCGGAAC	CATCTGCAGGCTGACATTGA

Supplementary Table 2. Serum lipid and glucose levels in *Apoe*$^{-/-}$ mice.

Groups	Cholesterol (mM)	Triglyceride (mM)	Glucose (mg/dl)
Scramble shRNA	15.47±3.54	1.07±0.19	168±23
Scramble shRNA+Metformin	14.10±3.24	0.98±0.18	170±30
lncRNA-ANRIL shRNA	13.53±2.98	1.17±0.21	167±31
lncRNA-ANRIL shRNA+Metformin	13.27±3.43	0.95±0.13	161±23

Male *Apoe*$^{-/-}$ mice were infected with adenovirus via injection of tail vein. Two weeks later, mice were fed with western diet and received metformin in drinking water for 4 weeks. At the end of experiments, all mice were sacrificed under anesthesia and serum levels of cholesterol, triglyceride, and glucose in all fasting mice were assayed. N is 10-15 in each group.

Supplementary Table 3. Plasma cytokine levels in *Apoe*$^{-/-}$ mice.

Groups	IL-1β (pg/ml)	IL-6 (pg/ml)
Scramble shRNA	166.21±8.19	134.62±5.86
Scramble shRNA+Metformin	157.64±6.55	137.13±8.01
lncRNA-ANRIL shRNA	148.73±7.16	126.32±6.68
lncRNA-ANRIL shRNA+Metformin	140.69±8.23	130.63±7.38

Male *Apoe*$^{-/-}$ mice were infected with adenovirus via injection of tail vein. Two weeks later, mice were fed with western diet and received metformin in drinking water for 4 weeks. At the end of experiments, all mice were sacrificed under anesthesia and serum levels of IL-1β and IL-6 were assayed. N is 10-15 in each group.

Supplementary Table 4. Demographic data for individuals with or without atherosclerosis.

ID	Gender	Ages (years old)	Stenosis (%)
1	Male	47	8%
2	Male	46	7%
3	Female	59	10%
4	Female	26	5%
5	Male	47	7%
6	Female	57	22%
7	Male	40	39%
8	Female	46	14%
9	Male	51	27%
10	Male	62	41%
11	Male	74	98%
12	Male	59	82%
13	Female	43	63%
14	Female	68	77%
15	Male	54	86%